www.czasopisma.pan.pl PAN www.journals.pan.pl

ARCHIVES of FOUNDRY ENGINEERING

DE GRUYTER OPEN

ISSN (2299-2944)
Volume 15
Issue 3/2015

DOI: 10.1515/afe-2015-0054

Published quarterly as the organ of the Foundry Commission of the Polish Academy of Sciences

29 – 34

Effect of Chromium on the Solidification Process and Microstructure of Vermicular Graphite Cast Iron

G. Gumienny *, M. Dondzbach, B. Kacprzyk
Department of Materials Engineering and Production Systems, Lodz University of Technology,
Stefanowskiego 1/15 Street, 90-924 Łódź, Poland
*Corresponding author. E-mail address: grzegorz.gumienny@p.lodz.pl

Received 15.05.2015; accepted in revised form 29.05.2015

Abstract

The paper presents the results of studies of the effect of chromium concentration on the solidification process, microstructure and selected properties of cast iron with vermicular graphite. The vermicular graphite cast iron was obtained by an Inmold process. Studies covered the cast iron containing chromium in a concentration at which graphite is still able to preserve its vermicular form. The effect of chromium on the temperature of eutectic crystallization and on the temperature of the start and end of austenite transformation was discussed. The conditions under which, at a predetermined chromium concentration, the vermicular graphite cast iron of a pearlitic matrix is obtained were presented, and the limit concentration of chromium was calculated starting from which partial solidification of the cast iron in a metastable system takes place. The effect of chromium on the hardness of cast iron, microhardness of individual phases and surface fraction of carbides was disclosed.

Keywords: Theory of crystallization, Vermicular graphite cast iron, Crystallization, TDA method

1. Introduction

In Poland, vermicular or compacted graphite cast iron is covered by the Polish Standard PN-EN 16079: 2012. The standard specifies five grades of this cast iron with a tensile strength of 300 to 500 MPa at an elongation from 2.0 to 0.5%, respectively (Table 1). The tensile properties given in Table 1 refer to castings with a wall thickness of up to 30 mm.

Table 1.
The grades of vermicular graphite cast iron according to PN-EN 16079:2012

Symbol	Mechanical properties			
	R_m, MPa min.	$R_{p0,2}$, MPa min.	A, % min.	HBW
EN-GJV-300	300	210	2.0	140 to 210
EN-GJV-350	350	245	1.5	160 to 220
EN-GJV-400	400	280	1.0	180 to 240
EN-GJV-450	450	315	1.0	200 to 250
EN-GJV-500	500	350	0.5	220 to 260

As specified by this standard, the microstructure of cast iron matrix changes from a predominantly ferritic (grade EN-GJV-300) to pearlitic (grade EN-GJV-500) [1]. Compared to grey cast

iron, the cast iron with vermicular graphite is characterized by higher strength and improved ductility. The microstructure of its matrix is less sensitive to the casting wall thickness. Compared to ductile iron with a spheroidal form of graphite, the vermicular graphite cast iron has lower coefficient of thermal expansion, but higher thermal conductivity, higher resistance to dynamic changes of temperature, higher damping capacity and castability. Due to these advantages, the cast iron with vermicular graphite finds a wide range of specific applications. The first utilitarian use of this cast iron was for the brake discs in high-speed railway systems. Currently, this material is mainly used for the construction of IC engine blocks, manifolds, and similar parts. Very interesting complex of properties offered by this cast iron is the object of intensive research and numerous publications [2-12]. There is a fairly large group of publications describing the possibility of obtaining ausferrite in the vermicular graphite cast iron, giving rise to the cast iron grades known as AVI or CAVI [13-17]. There are very few publications, however, which would discuss the effect of alloying elements on the microstructure and properties of cast iron with vermicular graphite [18-20]. The lack of any more precise data in this field has led the authors of this article to studies which are hoped to fill, at least partially, the gap in the information on this particular subject. So, the aim of this work was to study the effect of chromium on the solidification behaviour, microstructure and hardness as well as microhardness of vermicular graphite cast iron.

2. Research methodology

Chemical composition of the tested cast iron is shown in Table 2. The cast iron with 2.7% chromium concentration was investigated. With this level of chromium concentration, the graphite precipitates in cast iron still preserve their vermicular shape. The charge for the furnace consisted of special pig iron (the composition is shown in Table 3), FeSi75 ferrosilicon and technically pure chromium. Metal was melted in an electric medium-frequency induction crucible furnace of 30 kg capacity. The vermicularizing treatment of cast iron was done by an Inmold process. At 1480°C, the cast iron was poured into a sand mould with the gating system comprising a spherical reaction chamber of φ85 mm diameter. In this chamber, a Lamet® 5504 magnesium master alloy supplied by Elkem Norway was placed. The composition of the master alloy is shown in Table 4. Behind the reaction chamber there was a mixing chamber and a control chamber. In the thermal centre of control chamber, a PtRh10-Pt thermocouple was placed to record temperature changes during alloy cooling and solidification. This allowed, in turn, plotting the TDA curves. This method has been widely used in studies of the solidification process of various metals alloys [21-24]. Behind the control chamber there was a stepped test casting with dimensions shown in Figure 1.

Sulphur concentration was comprised in the range of 0.011 ÷ 0.019%, while phosphorus concentration was in the range of 0.053 ÷ 0.073%.

Table 2.
Chemical composition of the test cast iron

No.	Chemical composition, wt%					Eutectic carbon equivalent, C_E, %
	C	Si	Mn	Mg	Cr	
1.	3.28	2.13	0.03	0.020	0.03	3.94
2.	3.52	2.09	0.04	0.023	0.27	4.17
3.	3.39	2.43	0.04	0.020	0.53	4.14
4.	3.56	2.04	0.04	0.013	0.75	4.17
5.	3.45	2.33	0.04	0.023	0.96	4.11
6.	3.52	2.33	0.04	0.017	1.51	4.15
7.	3.56	2.24	0.05	0.018	1.89	4.16
8.	3.63	2.11	0.04	0.015	2.81	4.13

Table 3.
Chemical composition of special pig iron

Chemical composition, %				
C	Si	Mn	P	S
3.91	0.22	0.05	0.072	0.02

Table 4.
Chemical composition of the nodularising and inoculating master alloy

Chemical composition, wt%					
Si	Mg	Ca	La	Al	Fe
44÷48	5÷6	0.4÷0.6	0.25÷0.40	0.8÷1.2	rest

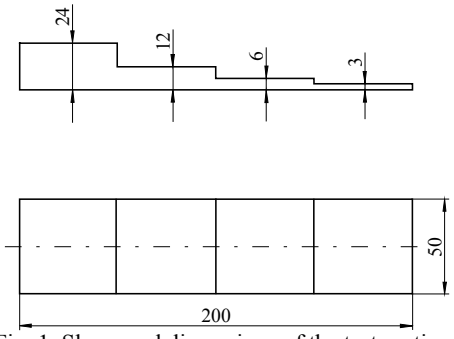

Fig. 1. Shape and dimensions of the test casting

Samples for metallographic examinations were cut out from the central part of the stepped casting. Metallographic examinations were carried out under a Nikon Eclipse MA200 optical microscope at a magnification of 500x. The surface fraction of carbides was examined by means of a NIS-Elements BR image analysis program. Hardness of cast iron was examined with an HPO-2400 durometer under the conditions of 2.5/187.5/15. Microhardness was measured with an HV-1000B microhardness tester under a load of 0.9807 N in accordance with PN EN ISO 6507-1.

3. Results

Figure 2 (a, b) shows the TDA curves plotted for an unalloyed vermicular graphite cast iron.

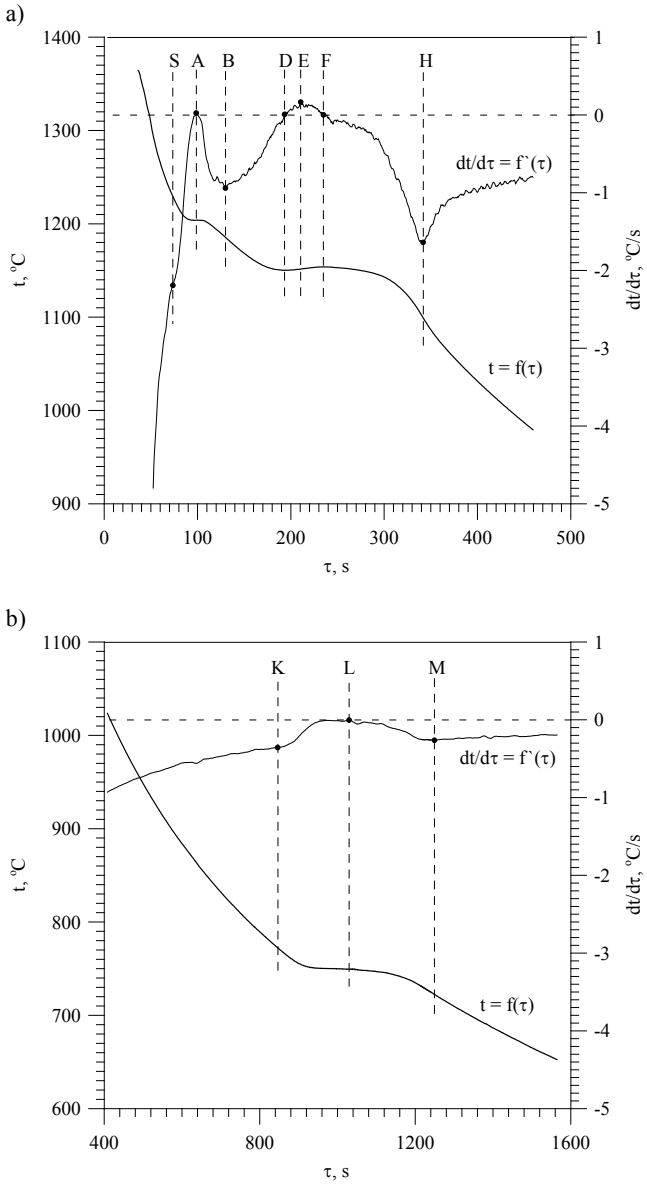

Fig. 2 (a, b). TDA curves of unalloyed vermicular graphite cast iron: a) the range of solidification, b) the range of austenite transformation

The solidification of cast iron started at 1229°C with the precipitation of austenite crystals. The thermal effect of this process is described by points SAB. Another thermal effect (points DEFH) comes from the crystallization of austenite + vermicular graphite eutectic. The solidification of cast iron ended at 1099°C (point H). The transformation of austenite began at a temperature of 772°C (point K, Fig. 2b) and ended at 722°C (point M, Fig. 2b).

With the addition of chromium introduced to the vermicular graphite cast iron, the number of thermal effects on the TDA curves has remained unchanged. What has changed were the coordinates of the points describing these effects. Therefore, Table 5 compares the coordinates of characteristic points on the TDA curves.

Table 5.
Temperature values at points describing the TDA curves of vermicular graphite cast iron

Cr concentration	t, °C							
	tS	tA	tB	tD	tF	tH	tK	tM
0.02	1229	1204	1186	1150	1154	1099	772	722
0.27	1192	1156	1151	1145	1149	1094	776	734
0.53	1210	1187	1172	1149	1150	1102	781	739
0.75	1202	1182	1169	1133	1140	1098	798	740
0.96	1175	1154	1150	1145	1148	1094	799	746
1.51	1212	1193	1171	1136	1146	1107	831	755
1.89	1209	1188	1176	1136	1138	1090	832	761
2.81	1205	1163	1155	1137	1137	1085	856	771

From the data compiled in Table 5 it follows that chromium reduces the temperature of eutectic crystallization by making the cast iron more prone to metastable crystallization (the values of temperature at points D, F and H) and raises the temperature of the $\gamma \rightarrow \alpha$ or $\gamma \rightarrow$ pearlite transformation (the temperature at points K and M). Figures 3 and 4 show the effect of chromium on the temperature of eutectic transformation and austenite decomposition.

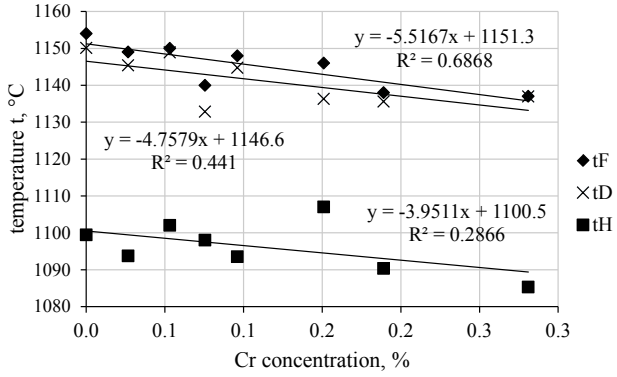

Fig. 3. Chromium concentration vs temperature of eutectic transformation

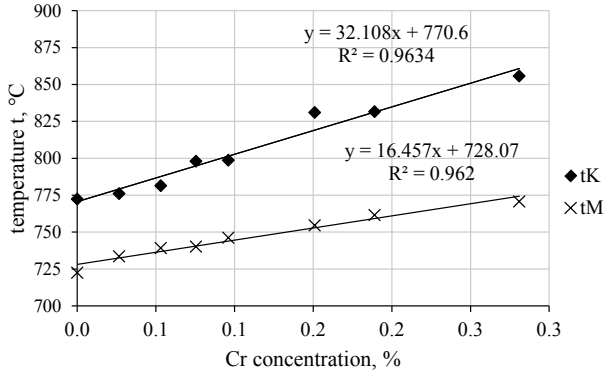

Fig. 4. Chromium concentration vs temperature of austenite transformation

Due to its antigraphitizing effect, chromium reduces the temperature of eutectic transformation (Table 5, Fig. 3). The data in Table 5 and Figure 4 show that chromium in the vermicular graphite cast iron raises the temperature of the beginning of solid-state transformation (tK) by about 32°C per each 1% Cr. The temperature of the end of austenite transformation (tM) rises with the increasing concentration of chromium by about 16.5°C per each 1% Cr over the entire examined range of chemical compositions. The extended range of eutectoid transformation testifies its lower rate due to carbon diffusion in austenite impeded by the presence of chromium.

Figure 5 (a, b) shows the microstructure of unalloyed vermicular graphite iron in castings with a wall thickness of 3 (a) and (b) 24 mm.

a)

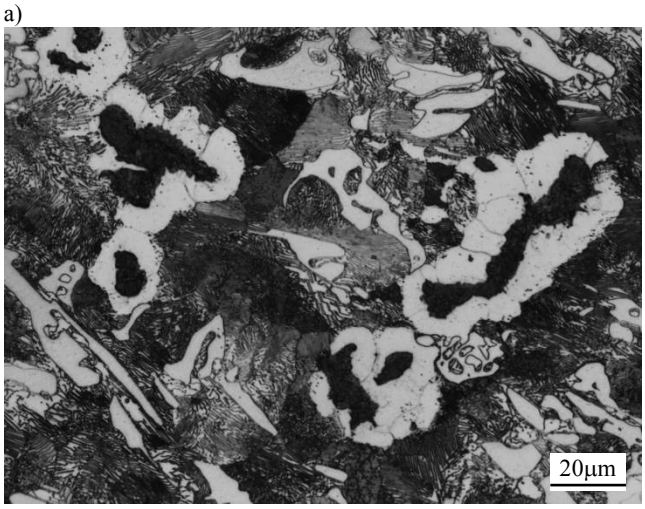

microstructure: vermicular graphite, pearlite, ferrite, cementite

b)

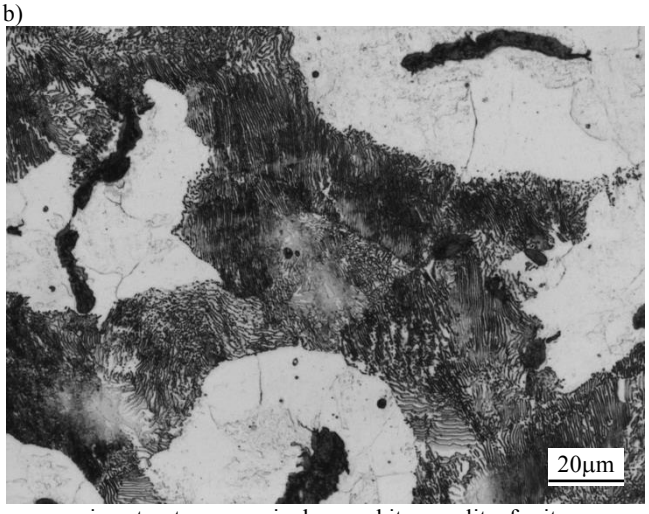

microstructure: vermicular graphite, pearlite, ferrite,

Fig. 5 (a, b). Microstructure of unalloyed vermicular graphite iron in castings with a wall thickness of: a) 3mm, b) 24 mm

Figure 5a shows that castings with a wall thickness of 3 mm contain precipitates of cementite formed due to the high cooling rate. Their surface fraction is 7.8%. The cast iron matrix is in prevailing part pearlitic with ferrite precipitates gathered around the vermicular graphite. An increase in the casting wall thickness results in the disappearance of Fe_3C carbide precipitates starting with the walls 6 mm thick and in the surface fraction of ferrite growing up to 50% in the walls of 24 mm thickness.

In the vermicular graphite iron castings with a wall thickness of 6 mm, chromium even in a concentration as low as 0.25% is already responsible for the formation of carbides. When this concentration is raised up to 0.75%, carbides are precipitating in the casting walls of both 12 and 24 mm thickness. The microstructure of vermicular graphite cast iron containing 0.75% Cr is shown in Figure 6 for the casting wall thickness of 24 mm.

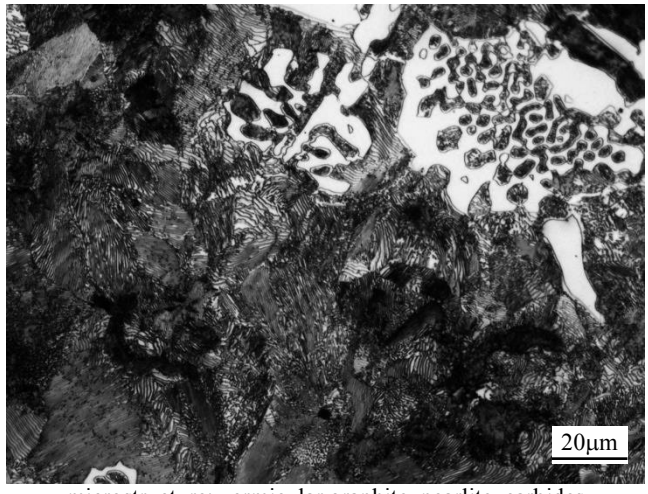

microstructure: vermicular graphite, pearlite, carbides

Fig. 6. Microstructure of vermicular graphite cast iron containing 0.75% Cr in castings with a wall thickness of 24 mm

Chromium content increased in cast iron has also increased the surface fraction of carbides as shown in Figure 7.

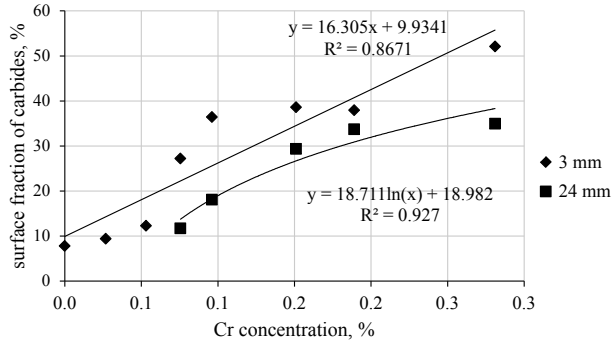

Fig. 7. Chromium concentration vs surface fraction of carbides in castings with a wall thickness of 3 and 24 mm

From Figure 7 it follows that surface fraction of carbides in the vermicular graphite iron castings with a wall thickness of

3 mm has been growing in an approximately proportional way from about 10% in unalloyed cast iron to about 52% in the cast iron containing 2.8% Cr. In castings with a wall thickness of 24 mm, carbides (~ 12%) were traced starting with the chromium concentration of 0.75%; their fraction was growing up to 35% in the cast iron containing 2.8% Cr.

In addition to the carbide-forming effect, chromium in the vermicular graphite cast iron has also a pearlite-forming effect. Loss of ferrite precipitates was observed with the chromium concentration of 0.75% in castings with a wall thickness from 3 to 12 mm. In castings with a wall thickness of 24 mm, trace amounts of ferrite were still observed when chromium concentration was at a level of 1% Cr.

Table 6 shows the results of hardness measurements taken on vermicular graphite iron castings and microhardness measurements of pearlite and carbides related to chromium concentration.

Table 6.
Hardness HB of the vermicular graphite cast iron and microhardness of pearlite and carbides

Cr concentration	Microhardness, μHV		Hardness HB of cast iron
	pearlite	carbides	
0.02	214	–	183
0.27	202	–	246
0.53	200	–	254
0.75	212	714	316
0.96	223	717	317
1.51	230	720	358
1.89	236	750	407
2.81	259	771	435

The effect of chromium concentration on hardness of the vermicular graphite cast iron and microhardness of pearlite and carbides is graphically shown in Figures 8-10.

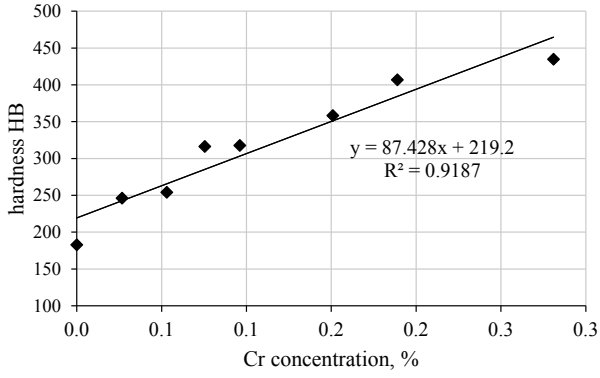

Fig. 8. Hardness of vermicular graphite cast iron vs chromium concentration

The plotted diagram shows that 1% Cr increases the cast iron hardness by about 87 HB units. This effect is roughly proportional over the entire examined range of chromium concentrations.

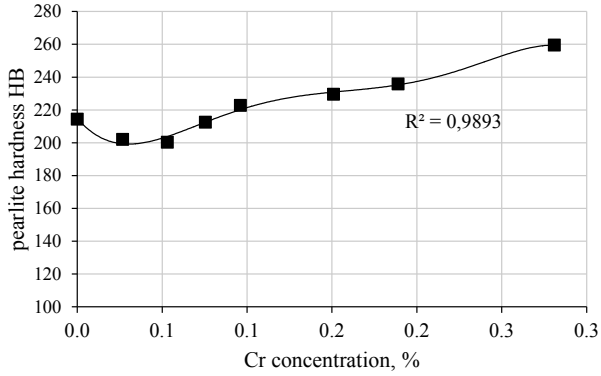

Fig. 9. Pearlite microhardness vs chromium concentration in vermicular graphite cast iron

Figure 9 shows that with chromium concentration of up to 0.5% pearlite hardness decreases, first, and increases next. This is probably due to the drop of ferrite hardness at a low chromium concentration [25]. The next increase in the eutectoid hardness is due to the hardness increase in both ferrite and cementite.

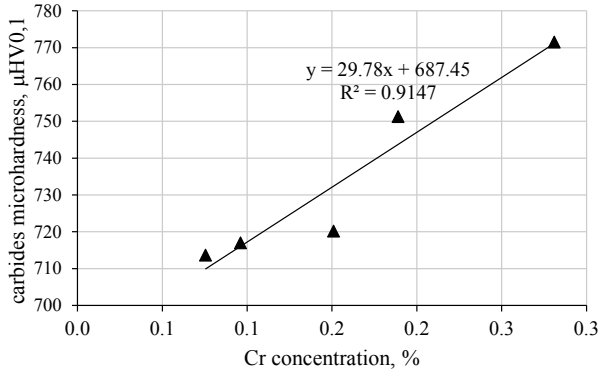

Fig. 10. Carbides microhardness vs chromium concentration in vermicular graphite cast iron

Figure 10 shows the increase of carbides microhardness roughly proportional to chromium concentration. Increasing chromium concentration by 1% has increased the hardness of isomorphous cementite by about 30 μHV units.

4. Conclusions

The data contained in this work enable drawing the following conclusions:

- chromium, by lowering the temperature of eutectic transformation, raises the temperature of the beginning and end of eutectoid transformation by 32°C and 16.5°C, respectively, per 1% of concentration,
- in the vermicular graphite cast iron obtained by an Inmold process, chromium causes complete pearlitization of the matrix at a 0.75% concentration in castings with a wall thick-

ness of 3-12 mm and at a 1.5% concentration in castings with a wall thickness of 24 mm,

- chromium raises the content of carbides in castings with a wall thickness of 3 mm from 10% in unalloyed cast iron to 52% in cast iron containing 2.8% Cr. In castings with a wall thickness of 24 mm, chromium shows its carbide-forming effect at a concentration of 0.75% raising the content of carbides from 12% (Cr ≅ 0.75%) up to 35% (Cr ≅ 2.8%),
- chromium in a concentration of 0.25-0.5% reduces the hardness of pearlite probably due to the ferrite hardness drop,
- chromium increases the hardness of cementite by about 30 HV0.1 units per 1% of concentration,
- chromium increases the hardness of vermicular graphite iron castings by about 87 HB units per 1% of concentration.

References

[1] Founding – Compacted (vermicular) graphite cast irons PN-EN 16079:2012.

[2] Pietrowski, S. (2000). Compendium of knowledge about vermicular cast iron. *Solidification of Metals and Alloys*. 2(44), 279-292. (in Polish).

[3] Guzik, E. (2010). Structure and mechanical properties as well as application of high quality vermicular cast iron. *Archives of Foundry Engineering.* 10(3), 95-100.

[4] Guzik, E. & Dzik, S. (2009). Structure and mechanical properties of vermicular cast iron in cylinder head casting. *Archives of Foundry Engineering.* 9*(*1), 175-180.

[5] Górny, M., Kawalec, M. & Sikora, G. (2014). Effect of Cooling Rate on Microstructure of Thin-Walled Vermicular Graphite Iron Castings. *Archives of Foundry Engineering*. 14(spec. 1), 139-142.

[6] Górny, M. & Kawalec, M. (2013). Role of Titanium in Thin Wall Vermicular Graphite Iron Castings Production. *Archives of Foundry Engineering*. 13(2), 25-28.

[7] Laneri, K., Bruna, P. & Crespo, D. Microstructural characterization and kinetics modelling of vermicular cast irons. Retrieved May, 25. 2015 from http://arxiv.org/ftp/cond-mat/papers/0606/0606031.pdf.

[8] Guzik, E. & Kleingartner, T. (2009). A study on the structure and mechanical properties of vermicular cast iron with pearlitic-ferritic matrix. *Archives of Foundry Engineering*. 9(3), 55-60.

[9] Kopyciński, D., Guzik, E., Nowak, A., Ronduda, M. & Sokolnicki, M. (2012). Preparation Vermicular Graphite in Thin and Thick Wall Iron Castings. *Archives of Foundry Engineering*. 12(2), 41-44.

[10] Pietrowski, S. (1998). A mechanism of the vermicular graphite crystallization in cast iron. *Solidification of Metals and Alloys.* 37, 97-104. (in Polish).

[11] Soiński, M.S. & Mierzwa, P. (2011). Effectiveness of cast iron vermicularization including 'conditioning' of the alloy. *Archives of Foundry Engineering*. 11(2). 133-138.

[12] Zych, J. & Żyrek, A. (2011). Vermicular cast iron production in the "Inmold" technology (in the Metalpol casting house) and the assessment of its thermal fatigue resistance *Archives of Foundry Engineering*. 11(spec. 3), 255-260.

[13] Mierzwa, P. & Soiński, M.S. (2010). The effect of thermal treatment on the mechanical properties of vermicular cast iron. *Archives of Foundry Engineering*. 10(spec. 1), 133-138.

[14] Andrsova, Z. & Volesky, L. (2012). The Potential of Isothermally Hardened Iron wth Vermicular Graphite. COMAT 2012. 21.-22. 11. 2012. Plzeň, Czech Republic, EU. Retrieved May, 25. 2015 from http://www.comat.cz/files/-proceedings/11/reports/1060.pdf.

[15] García-Hinojosa, J.A., Amaro A.M., Márquez, V.J. & Ramírez-Argaez, M.A. (2007). Manufacturing of Carbide Austempered Vermicular Iron. METAL 2007. 22. – 24. 5. 2007 Hradec nad Moravicí. Retrieved May, 25. 2015 from http://konsyst.tanger.cz/files/proceedings/metal_07/Lists/Papers/120.pdf.

[16] Pytel, A. & Gazda, A. (2014). Evaluation of selected properties in austempered vermicular cast iron (AVCI). *Transactions of Foundry Research Institute*. LIV(4), 23-31. DOI: 10.7356/iod.2014.18.

[17] Soiński, M.S. & Jakubus, A. (2014). Initial Assessment of Abrasive Wear Resistance of Austempered Cast Iron with Vermicular Graphite. Arch*ives of Metallurgy and Materials. 59*(3), 1073-1076. DOI: 10.2478/amm-2014-0183.

[18] Pietrowski, S. (1998). Alloyed Cast Iron with Vermicular Graphite. *Solidification of Metals and Alloys*. 37, 105-111. (in Polish).

[19] Choong-Hwan, L. & Byeong-Choon, G. (2011). Development of Compacted Vermicular Graphite Cast Iron for Railway Brake Discs. *Met. Mater. Int. 17*(2), 199-205.

[20] Popov, P.I. & Sizov, I.G. (2006). Effect of Alloying Elements on the Structure and Properties of Iron with Vermicular Graphite. *Metal Science and Heat Treatment.* 48(5-6), 272-275.

[21] Rapiejko, C., Pisarek, B., Czekaj, E. & Pacyniak, T. (2014). Analysis of the Crystallization of AZ91 Alloy by Thermal and Derivative Analysis Method Intensively Cooled in Ceramic Shell. *Archives of Foundry Engineering*. 14(1), 97-102.

[22] Pietrowski, S., Pisarek, B., Władysiak, R., Gumienny, G. & Szymczak, T. (2009). TDA curves of metals alloys and the control of their quality. In Szajnar J. *Advances in Theory and Practice Foundry*. (pp. 345-377). Katowice – Gliwice: PAN. (in Polish).

[23] Pisarek, B.P. (2013). Model of Cu-Al-Fe-Ni Bronze Crystallisation. *Archives of Foundry Engineering*. *13*(3), 72-79.

[24] Kacprzyk, B., Szymczak, T., Gumienny, G. & Klimek, L. (2013). Effect of the Remelting on Transformations in Co-Cr-Mo Prosthetics Alloy. *Archives of Foundry Engineering*. 13(3), 47-50.

[25] Dobrzański, L.A. (2004). *Metal engineering materials*. Warsaw: WNT. (in Polish).